

# An Entropic Solver for Ideal Lagrangian Magnetohydrodynamics

Fabienne Bezar<sup>\*</sup> and Bruno Després<sup>†</sup>

<sup>\*</sup>Dassault System, France; <sup>†</sup>Commissariat à l'Energie Atomique, BP 12, 91680 Bruyeres le Chatel, France, and Laboratoire d'Analyse Numérique, Université de Paris VI, 4 Place Jussieu, 75252 Paris, France  
E-mail: [despres@bruyeres.cea.fr](mailto:despres@bruyeres.cea.fr), [despres@ann.jussieu.fr](mailto:despres@ann.jussieu.fr)

Received September 29, 1998; revised April 8, 1999

---

In this paper, we adapt to the ideal 1D lagrangian MHD equations a class of numerical schemes of order one in time and space presented in an earlier paper and applied to the gas dynamics system. They use some properties of systems of conservation laws with zero entropy flux which describe fluid models invariant by galilean transformation and reversible for regular solutions. These numerical schemes satisfy an entropy inequality under CFL conditions. In the last section, we describe a particular scheme for the MHD equations and show with some numerical applications its robustness and accuracy. The generalization to full Eulerian multidimensional MHD will be the subject of a forthcoming paper. © 1999 Academic Press

*Key Words:* magnetohydrodynamics; finite difference methods.

---

## 1. INTRODUCTION

The MHD equations describe the flow of a conducting fluid in the presence of a magnetic field. The system is written in a conservative form and is hyperbolic with seven real eigenvalues. It presents three different waves: slow waves, Alfvén waves, and fast waves. Of course, this system shares similarities with the gas dynamics system. Nevertheless, its study is more difficult because it is neither strictly hyperbolic nor convex. The non-strict hyperbolicity means that the eigenvalues are not necessarily distinct. The non-convexity signifies that some waves are neither non-linear nor linearly degenerate. The question of the stability of these waves is more or less an open question at the present time, both from a theoretical and a numerical point of view. In spite of these difficulties, numerical schemes have been developed to solve this system. In many cases, these schemes are generalized schemes that were highly efficient for the equations of gas dynamics. We will mention a few approaches. Brio and Wu [5] proposed a Roe-type method but their technique required that the ratio of specific heats  $\gamma$  be equal to 2. Later, in the case of the lagrangian equations, Cargo *et al.* [8] studied a Roe matrix with the arithmetic average for any  $\gamma$ . Dai and Woodward [9, 10] proposed

an approximate method for solving the MHD Riemann problem. All these schemes are of Godunov-type. In this paper, we present a new class of numerical schemes [13] for some fluid systems and we generalize to MHD equations. These schemes are based on a new symmetrization result for Lagrangian systems (see also [4]). We demonstrate that the schemes are entropic under CFL conditions and positively conservative: this is detailed in Lemma 3.1. An interesting feature of these schemes is their simplicity in comparison with, for example, the Roe method [8–14]. In this work we restrict ourselves to one order schemes (in space and time) because they are better suited for a rigorous analysis than high order schemes. Nevertheless we think that the extension of our approach to high order schemes using standard techniques is straightforward. We also restrict to the one-dimensional case: it is sufficient in order to present the main features of our approach. We are now working on the extension to the multidimensional case. See also [16] for a quite different approach in the multidimensional case.

The plan of this paper is the following. In the first section, we will present general properties of systems of conservation laws with vanishing entropy flux. Then, we will show that the system of MHD equations satisfies such properties. In the second section, a class of schemes will be constructed and we mention in particular one scheme. Finally, we present numerical examples to illustrate the behavior of this lagrangian scheme. These results will be compared to other schemes. In the last section, we propose a summary with some discussions.

## 2. SYSTEMS OF CONSERVATION LAWS WITH VANISHING ENTROPY FLUX: APPLICATION TO THE MHD EQUATIONS

In a first step, we exhibit some properties of systems which describe fluid models invariant by galilean transformation and reversible for regular solutions [13]. Then, we will show that the system of lagrangian one-dimensional MHD equations belongs to this category of systems.

### 2.1. *Properties of Systems of Conservation Laws with Vanishing Entropy Flux*

We consider the system of conservation laws

$$\frac{\partial U}{\partial t} + \frac{\partial f(U)}{\partial m} = 0 \quad (1)$$

with  $U$  a vector of  $\mathbb{R}^d$ ,  $d \geq 1$ , and  $U \mapsto f(U)$  a smooth function defined from  $\mathbb{R}^d$  to  $\mathbb{R}^d$ . We suppose that, for this system (1), there exists an entropy  $\xi$  which is a strictly convex function of  $U$ . This function satisfies the inequality

$$\frac{d^2 \xi}{dU^2} > 0.$$

The vector  $U$  is also a solution of the system

$$\frac{\partial \xi(U)}{\partial t} + \frac{\partial F(U)}{\partial m} = 0,$$

where  $F(U)$  is called the entropy flux. We have the additional relation

$$\frac{\partial F(U)}{\partial U} = \left( \frac{d\xi}{dU} \right)^t \frac{df(U)}{dU}.$$

We suppose that for system (1), the entropy flux is vanishing, therefore

$$\left( \frac{d\xi}{dU} \right)^t \frac{df(U)}{dU} = 0.$$

Let us introduce the change of variables  $U \mapsto V(U)$  where

$$V = \frac{d\xi}{dU}.$$

One can write

$$\left( \frac{d\xi}{dU} \right)^t \frac{df(U)}{dU} = 0 \Leftrightarrow V^t \frac{df(U)}{dU} = 0 \Leftrightarrow V^t \frac{df(U)}{dV} \frac{dV}{dU} = 0.$$

As  $\xi$  is strictly convex, the change of variables  $U \mapsto V(U)$  is regular and the matrix  $\frac{dV}{dU}$  is invertible. We deduce that

$$V^t \frac{df(U)}{dV} = 0. \tag{2}$$

By applying a theorem from [15], we know that a necessary and sufficient condition for system (1) to possess a strictly convex entropy is that there exists a change of dependent variables that symmetrizes (1). The choice  $V = \frac{d\xi}{dU}$  ensures that the matrix  $\frac{df(U)}{dV}$  is symmetric and from (2), we obtain

$$\frac{df(U)}{dV} V = 0. \tag{3}$$

In the cases considered here, the last component  $V_d$  of  $V$  is non-zero. Thus we introduce the vector  $\Psi$  of  $\mathbb{R}^{d-1}$  defined by

$$\Psi = (\Psi_1, \dots, \Psi_{d-1})^t = \left( \frac{V_1}{V_d}, \dots, \frac{V_{d-1}}{V_d} \right)^t.$$

From Eq. (3), we deduce (see [13]) the existence of a function  $\tilde{f} : \mathbb{R}^{d-1} \rightarrow \mathbb{R}^{d-1}$  such that

$$f(U) = \tilde{f}(\Psi) = (\tilde{f}_1, \tilde{f}_2, \dots, \tilde{f}_d)^t.$$

We state the theorem

**THEOREM 2.1.** *The system of conservation laws (1) with vanishing entropy flux, which describes fluid models invariant by Galilean transformation and reversible for regular solutions can be written in the form*

$$\frac{\partial U}{\partial t} + \frac{\partial}{\partial m} \left( \begin{array}{c} M\Psi \\ -\frac{1}{2}\Psi^t M\Psi \end{array} \right) = 0, \tag{4}$$

where  $M$  is a constant matrix of  $\mathbb{R}^{d-1} \times \mathbb{R}^{d-1}$ .

*Proof.* The proof is given in [13]. ■

The vector  $U$  is composed of  $d$  variables. We can distinguish  $d - q - 1$  state variables,  $q$  speed variables, and 1 variable for total energy,

$$U = \begin{pmatrix} \left( \begin{array}{c} U_1 \\ \vdots \\ U_{d-q-1} \end{array} \right) \\ \left( \begin{array}{c} U_{d-q} \\ \vdots \\ U_{d-1} \end{array} \right) \\ U_d \end{pmatrix}.$$

It is shown in [13] that the matrix  $M$  connects state variables with speed variables and is written

$$M = \begin{pmatrix} 0 & N \\ N^t & 0 \end{pmatrix},$$

where  $N$  is a matrix of  $\mathbb{R}^{d-q-1} \times \mathbb{R}^q$ . The  $d - 1$  first equations of (4) make this connection explicit. The last line of this system (4) corresponds to the equation of energy.

## 2.2. The MHD Equations

The ideal MHD equations characterize the flow of a conducting fluid in the presence of a magnetic field [17]. They represent the coupling of fluid dynamical equations with Maxwell's equations and by neglecting displacement current, electrostatic force, viscosity effects, resistivity, and heat conduction, one obtains the following ideal MHD equations,

$$\frac{\partial}{\partial t} \begin{pmatrix} \rho \\ \mathbf{B} \\ \rho \mathbf{u} \\ \rho E \end{pmatrix} + \nabla \cdot \begin{pmatrix} \rho \mathbf{u} \\ \mathbf{B} \otimes \mathbf{u} - \mathbf{u} \otimes \mathbf{B} \\ \rho \mathbf{u} \otimes \mathbf{u} + p^* I - \frac{\mathbf{B} \otimes \mathbf{B}}{\mu} \\ (\rho E + p^*) \mathbf{u} - (\mathbf{u} \cdot \mathbf{B}) \frac{\mathbf{B}}{\mu} \end{pmatrix} = 0,$$

where  $\rho$  is the density,  $\mathbf{B} = (B_x, B_y, B_z)$  the magnetic field,  $\mathbf{u} = (u, v, w)$  the flow velocity,  $p$  the thermal pressure,  $p^* = p + \frac{\mathbf{B} \cdot \mathbf{B}}{2\mu}$  the total pressure, and  $\mu$  the magnetic permeability of vacuum. The total energy  $E$  is defined by  $\rho E = \rho \varepsilon + \frac{1}{2} \rho \mathbf{u} \cdot \mathbf{u} + \frac{\mathbf{B} \cdot \mathbf{B}}{2\mu}$  with  $\varepsilon$  the internal energy and the pressure  $p$  is related to the internal energy through the gamma-law equation of state

$$p = (\gamma - 1) \rho \varepsilon.$$

To this system, we must add the condition  $\operatorname{div}(\mathbf{B}) = 0$  on the magnetic field.

Under the one-dimensional approximation with plane symmetry, we obtain the following system of conservation laws,

$$\frac{\partial}{\partial t} \begin{pmatrix} \rho \\ B_y \\ B_z \\ \rho u \\ \rho v \\ \rho w \\ \rho E \end{pmatrix} + \frac{\partial}{\partial x} \begin{pmatrix} \rho u \\ u B_y - v B_x \\ u B_z - w B_x \\ \rho u^2 + P^* I \\ \rho u v - \frac{B_x B_y}{\mu} \\ \rho u w - \frac{B_x B_z}{\mu} \\ (\rho E + p^*)u - \frac{B_x(B_y v + B_z w)}{\mu} \end{pmatrix} = 0 \quad (5)$$

with  $B_x$ , the  $x$ -component of the magnetic field constant to satisfy the condition  $\text{div}(\mathbf{B}) = 0$ . We introduce a lagrangian mass coordinate  $m$  by the relation  $dm = \rho dx$  and we obtain the one-dimensional ideal MHD equations in mass coordinate

$$\frac{\partial}{\partial t} \begin{pmatrix} \tau \\ \tau B_y \\ \tau B_z \\ u \\ v \\ w \\ E \end{pmatrix} + \frac{\partial}{\partial m} \begin{pmatrix} -u \\ -B_x v \\ -B_x w \\ P_* \\ -\frac{B_x B_y}{\mu} \\ -\frac{B_x B_z}{\mu} \\ u P_* - \frac{B_x}{\mu} (B_y v + B_z w) \end{pmatrix} = 0. \quad (6)$$

Here,  $\tau = \frac{1}{\rho}$  is the specific volume of the fluid and we define

$$P_* = p + \frac{-B_x^2 + B_y^2 + B_z^2}{2\mu} = p^* - \frac{B_x^2}{\mu}.$$

For the ideal MHD equations, there exists a function entropy  $\xi(\tau, \varepsilon)$  strictly convex [21] and a function temperature  $T(\tau, \varepsilon)$  positive such that

$$-T d\xi = d\varepsilon + p d\tau$$

and from  $\varepsilon = E - \frac{1}{2} \mathbf{u} \cdot \mathbf{u} - \frac{\tau}{2\mu} \mathbf{B} \cdot \mathbf{B}$ , we obtain

$$-T d\xi = dE - u du - v dv - w dw - \frac{B_y}{\mu} d(\tau B_y) - \frac{B_z}{\mu} d(\tau B_z) + P_* d\tau. \quad (7)$$

For a regular solution of (6), we obtain easily that  $T \frac{\partial \xi}{\partial t} = 0$  and an entropic solution of (6) satisfies  $\frac{\partial \xi}{\partial t} \leq 0$ . In the case of an ideal gas, the entropy is  $\xi = p\tau^\gamma$ . Furthermore, for this system, the entropy flux is zero

$$\forall U, \quad \left( \frac{d\xi}{dU} \right)^t \frac{df(U)}{dU} = 0. \quad (8)$$

The system of MHD equations is invariant by galilean transformation (cf. [17]) and reversible for regular solutions. Consequently, it satisfies the hypothesis of Theorem 2.1. We can now exhibit the vectors  $V \in \mathbb{R}^7$ ,  $\Psi \in \mathbb{R}^6$ , and the matrix  $M \in \mathbb{R}^6 \times \mathbb{R}^6$  for the system of MHD equations in one dimension. From Eqs. (7) and (6), we deduce that

$$V = \frac{1}{T} \begin{pmatrix} -P_* \\ \frac{B_y}{\mu} \\ \frac{B_z}{\mu} \\ u \\ v \\ w \\ -1 \end{pmatrix}. \quad (9)$$

It is easy to see that Eq. (6) is of type (4) setting

$$\Psi = \begin{pmatrix} P_* \\ -\frac{B_y}{\mu} \\ -\frac{B_z}{\mu} \\ -u \\ -v \\ -w \end{pmatrix} \quad \text{and} \quad M = \begin{pmatrix} 0 & 0 & 0 & 1 & 0 & 0 \\ 0 & 0 & 0 & 0 & B_x & 0 \\ 0 & 0 & 0 & 0 & 0 & B_x \\ 1 & 0 & 0 & 0 & 0 & 0 \\ 0 & B_x & 0 & 0 & 0 & 0 \\ 0 & 0 & B_x & 0 & 0 & 0 \end{pmatrix}. \quad (10)$$

For the MHD equations, the state variables are  $\tau$ ,  $\tau B_y$ ,  $\tau B_z$  [17] and the speed variables  $u$ ,  $v$ ,  $w$ . The matrix  $M$  can be written

$$M = \begin{pmatrix} 0 & N \\ N^t & 0 \end{pmatrix}$$

with  $N$  a square diagonal matrix of  $\mathbb{R}^3 \times \mathbb{R}^3$  given by

$$N = \begin{pmatrix} 0 & 0 & 0 \\ 0 & B_x & 0 \\ 0 & 0 & B_x \end{pmatrix}.$$

The couples of variables  $(u, P_*)$ ,  $(v, B_y)$ , and  $(w, B_z)$  are directly connected. This particular connection will be the basis of the numerical scheme.

### 3. A CLASS OF NUMERICAL SCHEMES

In this section, we present the main features of a new class of numerical schemes for systems of conservation laws which satisfy (1) and (2). These schemes satisfy good entropy properties under CFL conditions. Then, we describe a particular scheme for the one-dimensional lagrangian MHD equations.

#### 3.1. Construction of the Scheme

We consider a mesh  $(\Omega_j)$  of  $\mathbb{R}$  with  $\Omega_j = [m_{j-1/2}, m_{j+1/2}]$ . The length of each segment  $\Omega_j$  is  $\Delta m_j = m_{j+1/2} - m_{j-1/2}$ . The quantities  $U_j^n$  or  $\Psi_j^n$  are mean values of  $U$  or  $\Psi$  defined

at the center of cell  $\Omega_j$  at time  $t_n$ . Following a finite volume approach, we integrate Eq. (1) in the cell  $\Omega_j$ :

$$\int_{\Omega_j} \frac{\partial U}{\partial t} dm + f(U)_{j+\frac{1}{2}}^n - f(U)_{j-\frac{1}{2}}^n = 0.$$

A time discretization of order 1 gives

$$U_j^{n+1} - U_j^n = -\frac{\Delta t}{\Delta m_j} \left( f(U)_{j+\frac{1}{2}}^n - f(U)_{j-\frac{1}{2}}^n \right). \quad (11)$$

So, we have to evaluate  $f(U)_{j+1/2}^n$  to write the scheme completely. To do this, we use the particular form (4). We introduce the following definition

**DEFINITION 3.1.** A Sylvester decomposition of a matrix  $M$  is defined by  $p$  reals  $(\mu_i)_{i=1\dots p}$  and  $p$  vectors  $(l_i)_{i=1\dots p}$  such that

$$M = \sum_{i=1}^{i=p} \mu_i l_i l_i^t.$$

This decomposition is not unique and  $P \leq p \leq +\infty$  where  $P$  is the number of eigenvalues of  $M$  distinct from 0.

So, at the interface between cell  $\Omega_j$  and cell  $\Omega_{j+1}$ , the matrix  $M$  can be written under the form

$$M_{j+\frac{1}{2}} = \sum_{i=1}^{i=p} \mu_{i,j+\frac{1}{2}} l_{i,j+\frac{1}{2}} l_{i,j+\frac{1}{2}}^t$$

and the numerical flux becomes

$$f(U)_{j+\frac{1}{2}}^n = \left( \begin{array}{l} \sum_{\mu_{i,j+\frac{1}{2}} < 0} \mu_{i,j+\frac{1}{2}} (\Psi_j^n \cdot l_{i,j+\frac{1}{2}}) l_{i,j+\frac{1}{2}} + \sum_{\mu_{i,j+\frac{1}{2}} > 0} \mu_{i,j+\frac{1}{2}} (\Psi_{j+1}^n \cdot l_{i,j+\frac{1}{2}}) l_{i,j+\frac{1}{2}} \\ -\frac{1}{2} \left( \sum_{\mu_{i,j+\frac{1}{2}} < 0} \mu_{i,j+\frac{1}{2}} (\Psi_j^n \cdot l_{i,j+\frac{1}{2}})^2 + \sum_{\mu_{i,j+\frac{1}{2}} > 0} \mu_{i,j+\frac{1}{2}} (\Psi_{j+1}^n \cdot l_{i,j+\frac{1}{2}})^2 \right) \end{array} \right), \quad (12)$$

where the first line is a vector of  $\mathbb{R}^{d-1}$  and the second one a real of  $\mathbb{R}$ . This flux is consistent and is upwinded according to the sign of  $\mu_{i,j+1/2}$ .

### 3.2. Entropic Schemes

In this section, we demonstrate that under a CFL condition, this class of schemes is entropic. In the whole paper we use the mathematical convex entropy  $\xi$ : for MHD and many other problems  $\xi$  is the opposite of the physical concave entropy  $\xi = -S$ . This is detailed in the following. We also assume in the proof that  $V_d < 0$ . This is not a restriction

and is compatible with physical situations we are interested in since  $V_d = -\frac{1}{T} < 0$ , where  $T > 0$  is the physical temperature.

LEMMA 3.1. *There exists a constant  $C_j^n > 0$  such that if*

$$C_j^n \frac{\Delta t}{\Delta m_j} < 1, \quad (13)$$

then

$$\xi(U_j^{n+1}) \leq \xi(U_j^n).$$

*Remark 3.1.* Theoretical analysis of the constant  $C_j^n$  shows that this constant is always greater than or equal to the maximum eigenvalue of the Jacobian matrix. We refer to [13] for the complete analysis, which is rather technical. In practice we always do as if this constant is equal to the maximum eigenvalue of the Jacobian matrix. It is the case for the scheme we introduce in the following Subsection 3.3.

*Proof.* We define  $U(\alpha)$  by  $U(\alpha) = U_j^n + \alpha(U_j^{n+1} - U_j^n)$  for  $\alpha \in [0, 1]$ . Thus, we obtain  $\xi(U(0)) = \xi(U_j^n)$  and  $\xi(U(1)) = \xi(U_j^{n+1})$ . We make a Taylor expansion of  $\xi$  between  $U(0)$  and  $U(1)$ . There exists  $\alpha_0 \in [0, 1]$  such that

$$\xi(U(0)) = \xi(U(1)) - \frac{d\xi(U(\alpha))}{d\alpha}(1) + \frac{1}{2} \frac{d^2\xi(U(\alpha))}{d\alpha^2}(\alpha_0). \quad (14)$$

The term  $(1/2)(d^2\xi(U(\alpha))/d\alpha^2)(\alpha_0)$  can be written

$$\frac{1}{2} \frac{d^2\xi(U(\alpha))}{d\alpha^2}(\alpha_0) = \frac{1}{2} \frac{d}{d\alpha} \left( \frac{d\xi}{dU} \frac{dU(\alpha)}{d\alpha} \right) (\alpha_0).$$

Knowing that  $\frac{dU(\alpha)}{d\alpha} = U_j^{n+1} - U_j^n$ , we deduce

$$\frac{1}{2} \frac{d^2\xi(U(\alpha))}{d\alpha^2}(\alpha_0) = \frac{1}{2} (U_j^{n+1} - U_j^n)^t \frac{d^2\xi}{dU^2}(\alpha_0) (U_j^{n+1} - U_j^n).$$

As  $\xi$  is a strictly convex function of  $U$ , the left-hand side is a quadratic form  $Q_1$  definite positive such that

$$\frac{1}{2} \frac{d^2\xi(U(\alpha))}{d\alpha^2}(\alpha_0) = Q_1 (U_j^{n+1} - U_j^n).$$

We have now to look at the term  $\frac{d\xi(U(\alpha))}{d\alpha}(1)$  of (14),

$$\begin{aligned} \frac{d\xi(U(\alpha))}{d\alpha}(1) &= \frac{d\xi}{dU} \frac{dU(\alpha)}{d\alpha}(1) \\ &= (V_j^{n+1})^t (U_j^{n+1} - U_j^n) \\ &= -(V_j^{n+1})^t \frac{\Delta t}{\Delta m_j} \left( f(U)_{j+\frac{1}{2}}^n - f(U)_{j-\frac{1}{2}}^n \right). \end{aligned}$$



With the decomposition (12), we obtain

$$\begin{aligned}
& -(V_j^{n+1})^t \left( f(U)_{j+\frac{1}{2}}^n - f(U)_{j-\frac{1}{2}}^n \right) = -(V_d)_j^{n+1} \left( \Psi_j^{n+1,t} \left[ \sum_{\mu_{i,j+\frac{1}{2}} < 0} \mu_{i,j+\frac{1}{2}} \left( l_{i,j+\frac{1}{2}} \cdot \Psi_j^n \right) l_{i,j+\frac{1}{2}} \right. \right. \\
& \left. \left. + \sum_{\mu_{i,j+\frac{1}{2}} > 0} \mu_{i,j+\frac{1}{2}} \left( l_{i,j+\frac{1}{2}} \cdot \Psi_{j+1}^n \right) l_{i,j+\frac{1}{2}} \right] \right. \\
& \left. - \Psi_j^{n+1,t} \left[ \sum_{\mu_{i,j-\frac{1}{2}} < 0} \mu_{i,j-\frac{1}{2}} \left( l_{i,j-\frac{1}{2}} \cdot \Psi_{j-1}^n \right) l_{i,j-\frac{1}{2}} + \sum_{\mu_{i,j-\frac{1}{2}} > 0} \mu_{i,j-\frac{1}{2}} \left( l_{i,j-\frac{1}{2}} \cdot \Psi_j^n \right) l_{i,j-\frac{1}{2}} \right] \right. \\
& \left. - \frac{1}{2} \left( \sum_{\mu_{i,j+\frac{1}{2}} < 0} \mu_{i,j+\frac{1}{2}} \left( l_{i,j+\frac{1}{2}} \cdot \Psi_j^n \right)^2 + \sum_{\mu_{i,j+\frac{1}{2}} > 0} \mu_{i,j+\frac{1}{2}} \left( l_{i,j+\frac{1}{2}} \cdot \Psi_{j+1}^n \right)^2 \right) \right. \\
& \left. + \frac{1}{2} \left( \sum_{\mu_{i,j-\frac{1}{2}} < 0} \mu_{i,j-\frac{1}{2}} \left( l_{i,j-\frac{1}{2}} \cdot \Psi_{j-1}^n \right)^2 + \sum_{\mu_{i,j-\frac{1}{2}} > 0} \mu_{i,j-\frac{1}{2}} \left( l_{i,j-\frac{1}{2}} \cdot \Psi_j^n \right)^2 \right) \right).
\end{aligned}$$

In (9), we have  $V_7 = -\frac{1}{T} < 0$ . Then, using the fact that  $(V_d)_j^{n+1} < 0$  in the physical situations we are interested in and using the inequality  $ab < \frac{1}{2}(a^2 + b^2)$  in the second term of the first line and in the first one of the second line, we have the inequality

$$\begin{aligned}
& -(V_j^{n+1})^t \left( f(U)_{j+\frac{1}{2}}^n - f(U)_{j-\frac{1}{2}}^n \right) \\
& \leq -\frac{1}{2} (V_d)_j^{n+1} \left( \sum_{\mu_{i,j+\frac{1}{2}} < 0} (-\mu_{i,j+\frac{1}{2}}) \left( \left[ l_{i,j+\frac{1}{2}} \cdot (\Psi_j^n - \Psi_j^{n+1}) \right]^2 \right. \right. \\
& \left. \left. - \left[ l_{i,j+\frac{1}{2}} \cdot \Psi_j^n \right]^2 - \left[ l_{i,j+\frac{1}{2}} \cdot \Psi_j^{n+1} \right]^2 \right) \right. \\
& \left. + \sum_{\mu_{i,j+\frac{1}{2}} > 0} \mu_{i,j+\frac{1}{2}} \left( \left[ l_{i,j+\frac{1}{2}} \cdot \Psi_{j+1}^n \right]^2 + \left[ l_{i,j+\frac{1}{2}} \cdot \Psi_j^{n+1} \right]^2 \right) \right. \\
& \left. + \sum_{\mu_{i,j-\frac{1}{2}} < 0} (-\mu_{i,j-\frac{1}{2}}) \left( \left[ l_{i,j-\frac{1}{2}} \cdot \Psi_{j-1}^n \right]^2 + \left[ l_{i,j-\frac{1}{2}} \cdot \Psi_j^{n+1} \right]^2 \right) \right. \\
& \left. + \sum_{\mu_{i,j-\frac{1}{2}} > 0} (\mu_{i,j-\frac{1}{2}}) \left( \left[ l_{i,j-\frac{1}{2}} \cdot (\Psi_j^n - \Psi_j^{n+1}) \right]^2 - \left[ l_{i,j-\frac{1}{2}} \cdot \Psi_j^n \right]^2 - \left[ l_{i,j-\frac{1}{2}} \cdot \Psi_j^{n+1} \right]^2 \right) \right. \\
& \left. + \sum_{\mu_{i,j+\frac{1}{2}} < 0} (-\mu_{i,j+\frac{1}{2}}) \left( l_{i,j+\frac{1}{2}} \cdot \Psi_j^n \right)^2 - \sum_{\mu_{i,j+\frac{1}{2}} > 0} \mu_{i,j+\frac{1}{2}} \left( l_{i,j+\frac{1}{2}} \cdot \Psi_{j+1}^n \right)^2 \right. \\
& \left. + \sum_{\mu_{i,j-\frac{1}{2}} < 0} \mu_{i,j-\frac{1}{2}} \left( l_{i,j-\frac{1}{2}} \cdot \Psi_{j-1}^n \right)^2 + \sum_{\mu_{i,j-\frac{1}{2}} > 0} \mu_{i,j-\frac{1}{2}} \left( l_{i,j-\frac{1}{2}} \cdot \Psi_j^n \right)^2 \right).
\end{aligned}$$

We use

$$\begin{aligned}
& \sum_{\mu_{i,j+\frac{1}{2}} < 0} \mu_{i,j+\frac{1}{2}} \left[ l_{i,j+\frac{1}{2}} \cdot \Psi_j^{n+1} \right]^2 + \sum_{\mu_{i,j+\frac{1}{2}} > 0} \mu_{i,j+\frac{1}{2}} \left[ l_{i,j+\frac{1}{2}} \cdot \Psi_j^{n+1} \right]^2 \\
& + \sum_{\mu_{i,j-\frac{1}{2}} < 0} (-\mu_{i,j-\frac{1}{2}}) \left[ l_{i,j-\frac{1}{2}} \cdot \Psi_j^{n+1} \right]^2 - \sum_{\mu_{i,j-\frac{1}{2}} > 0} \mu_{i,j-\frac{1}{2}} \left[ l_{i,j-\frac{1}{2}} \cdot \Psi_j^{n+1} \right]^2 \\
& = (\Psi_j^{n+1})^t M \Psi_j^{n+1} - (\Psi_j^{n+1})^t M \Psi_j^{n+1} = 0.
\end{aligned}$$

It follows that

$$\begin{aligned}
& -(V_j^{n+1})^t \left( f(U)_{j+\frac{1}{2}}^n - f(U)_{j-\frac{1}{2}}^n \right) \\
& \leq -\frac{1}{2} (V_d)_j^{n+1} \left( \sum_{\mu_{i,j+\frac{1}{2}} < 0} (-\mu_{i,j+\frac{1}{2}}) \left[ l_{i,j+\frac{1}{2}} \cdot (\Psi_j^n - \Psi_j^{n+1}) \right]^2 \right. \\
& \quad \left. + \sum_{\mu_{i,j-\frac{1}{2}} > 0} \mu_{i,j-\frac{1}{2}} \left[ l_{i,j-\frac{1}{2}} \cdot (\Psi_j^n - \Psi_j^{n+1}) \right]^2 \right).
\end{aligned}$$

We know that  $(V_d)_j^{n+1} < 0$ , thus we deduce that there exists a quadratic form  $\mathcal{Q}_2$  definite positive such that

$$-(V_j^{n+1})^t \left( f(U)_{j+\frac{1}{2}}^n - f(U)_{j-\frac{1}{2}}^n \right) \leq \mathcal{Q}_2(\Psi_j^n - \Psi_j^{n+1}).$$

Furthermore, we define the quadratic form  $\mathcal{Q}_3$  such that  $\mathcal{Q}_3(U_j^{n+1} - U_j^n) = \mathcal{Q}_2(\Psi_j^{n+1} - \Psi_j^n)$ . We come back to Eq. (14) and write

$$\xi(U_j^n) - \xi(U_j^{n+1}) \geq \left( -\mathcal{Q}_3 \frac{\Delta t}{\Delta m_j} + \mathcal{Q}_1 \right) (U_j^n - U_j^{n+1}).$$

As soon as we have the positivity of  $-\mathcal{Q}_3(\Delta t / \Delta m_j) + \mathcal{Q}_1$ , the scheme satisfies an entropy inequality. If we choose

$$C_j^n = \sup_{U \in \mathbb{R}^d} \left( \frac{|\mathcal{Q}_3(U)|}{\mathcal{Q}_1(U)} \right),$$

under the condition

$$C_j^n \frac{\Delta t}{\Delta m_j} < 1,$$

the scheme is entropic. ■

**PROPERTY 3.1.** *If condition (13) is satisfied, then specific volume and pressure calculated by the scheme remain positive, in the case of an ideal gas.*

*Proof.* Since the scheme is entropic under a CFL condition, we have  $\xi(U_j^{n+1}) \leq \xi(U_j^n)$ . So, in the case of an ideal gas,  $\varepsilon_j^0(\tau_j^0)^{\gamma-1} \leq \varepsilon_j^n(\tau_j^n)^{\gamma-1} \leq \varepsilon_j^{n+1}(\tau_j^{n+1})^{\gamma-1}$ . It follows that  $\varepsilon_j^n > 0$  and  $\tau_j^n > 0$  for each  $(j, n)$ . ■

### 3.3. A Particular Scheme for the MHD Equations

The matrix  $M$  is written

$$M = \begin{pmatrix} 0 & N \\ N^t & 0 \end{pmatrix}$$

with  $N = (n_{i,j})_{1 \leq i, j \leq 3}$  a square matrix of  $\mathbb{R}^3 \times \mathbb{R}^3$ . We decompose  $M$  with 18 reals  $\mu_k$  and associated vectors  $l_k$ . For each  $(i, j) \in \{1 \dots 3\}^2$  and for  $k = i + 3 \times j$ , we choose

$$\mu_k = \frac{n_{i,j}}{2}, \quad \mu_{k+9} = -\frac{n_{i,j}}{2}$$

and

$$l_k = \begin{pmatrix} 0 \\ \dots \\ 1 \\ 0 \\ \dots \\ 1 \\ 0 \\ \dots \end{pmatrix}, \quad l_{k+9} = \begin{pmatrix} 0 \\ \dots \\ 1 \\ 0 \\ \dots \\ -1 \\ 0 \\ \dots \end{pmatrix}.$$

The non-zero terms are the  $i$ th and the  $(j + 3)$ rd components of the vectors. We check that these vectors  $l_k$  and the coefficients  $\mu_k$  define a Sylvester decomposition of such a matrix  $M$ . In this section, we present an example of a scheme for the MHD equations using a particular Sylvester decomposition of matrix  $M$ . If we suppose that  $B_x \neq 0$ , then matrix  $M$  has 6 non-zero terms; therefore we can use the preceding decomposition introducing three reals  $C_1, C_2, C_3$  strictly positive which correspond to some physical speeds in lagrangian coordinates. In the case where  $B_x \neq 0$ , we propose a Sylvester decomposition with

$$\mu_1 = 1, \mu_2 = -1, \mu_3 = B_x, \mu_4 = -B_x, \mu_5 = B_x, \mu_6 = -B_x,$$

and the vectors

$$l_1 = \begin{pmatrix} -\frac{1}{\sqrt{2C_1}} \\ 0 \\ 0 \\ -\sqrt{\frac{C_1}{2}} \\ 0 \\ 0 \end{pmatrix}, \quad l_2 = \begin{pmatrix} \frac{1}{\sqrt{2C_1}} \\ 0 \\ 0 \\ -\sqrt{\frac{C_1}{2}} \\ 0 \\ 0 \end{pmatrix},$$

$$\begin{aligned}
 l_3 &= \begin{pmatrix} 0 \\ \sqrt{\frac{|B_x|\mu}{2C_2}} \\ 0 \\ 0 \\ \sqrt{\frac{C_2}{2\mu|B_x|}} \\ 0 \end{pmatrix}, & l_4 &= \begin{pmatrix} 0 \\ \sqrt{\frac{|B_x|\mu}{2C_2}} \\ 0 \\ 0 \\ -\sqrt{\frac{C_2}{2\mu|B_x|}} \\ 0 \end{pmatrix}, \\
 l_5 &= \begin{pmatrix} 0 \\ 0 \\ \sqrt{\frac{|B_x|\mu}{2C_3}} \\ 0 \\ 0 \\ \sqrt{\frac{C_3}{2\mu|B_x|}} \end{pmatrix}, & l_6 &= \begin{pmatrix} 0 \\ 0 \\ \sqrt{\frac{|B_x|\mu}{2C_3}} \\ 0 \\ 0 \\ -\sqrt{\frac{C_3}{2\mu|B_x|}} \end{pmatrix}.
 \end{aligned}$$

In the case where  $B_x = 0$ , we propose the following Sylvester decomposition with

$$\mu_1 = 1, \mu_2 = -1, \mu_3 = 1, \mu_4 = -1, \mu_5 = 1, \mu_6 = -1,$$

and the vectors

$$\begin{aligned}
 l_1 &= \begin{pmatrix} -\frac{1}{\sqrt{2C_1}} \\ 0 \\ 0 \\ -\sqrt{\frac{C_1}{2}} \\ 0 \\ 0 \end{pmatrix}, & l_2 &= \begin{pmatrix} \frac{1}{\sqrt{2C_1}} \\ 0 \\ 0 \\ -\sqrt{\frac{C_1}{2}} \\ 0 \\ 0 \end{pmatrix}, \\
 l_3 &= \begin{pmatrix} 0 \\ 0 \\ 0 \\ 0 \\ \sqrt{\frac{C_2}{2\mu}} \\ 0 \end{pmatrix}, & l_4 &= \begin{pmatrix} 0 \\ 0 \\ 0 \\ 0 \\ -\sqrt{\frac{C_2}{2\mu}} \\ 0 \end{pmatrix}, \\
 l_5 &= \begin{pmatrix} 0 \\ 0 \\ 0 \\ 0 \\ 0 \\ \sqrt{\frac{C_3}{2\mu}} \end{pmatrix}, & l_6 &= \begin{pmatrix} 0 \\ 0 \\ 0 \\ 0 \\ 0 \\ -\sqrt{\frac{C_3}{2\mu}} \end{pmatrix}.
 \end{aligned}$$

In both cases, we check that

$$M = \sum_{i=1}^{i=6} \mu_i l_i l_i^t.$$

If we come back to the equations of MHD, the numerical flux is

$$\left\{ \begin{array}{l} (f_1)_{j+\frac{1}{2}}^n = -\frac{(P_{*j}^n + C_{1,j+\frac{1}{2}} u_j^n) - (P_{*j+1}^n - C_{1,j+\frac{1}{2}} u_{j+1}^n)}{2C_{1,j+\frac{1}{2}}} \\ (f_2)_{j+\frac{1}{2}}^n = -B_x \frac{(-B_x B_{yj}^n + C_{2,j+\frac{1}{2}} v_j^n) - (-B_x B_{yj+1}^n - C_{2,j+\frac{1}{2}} v_{j+1}^n)}{2C_{2,j+\frac{1}{2}}} \\ (f_3)_{j+\frac{1}{2}}^n = -B_x \frac{(-B_x B_{zj}^n + C_{3,j+\frac{1}{2}} w_j^n) - (-B_x B_{zj+1}^n - C_{3,j+\frac{1}{2}} w_{j+1}^n)}{2C_{3,j+\frac{1}{2}}} \\ (f_4)_{j+\frac{1}{2}}^n = \frac{(P_{*j}^n + C_{1,j+\frac{1}{2}} u_j^n) + (P_{*j+1}^n - C_{1,j+\frac{1}{2}} u_{j+1}^n)}{2} \\ (f_5)_{j+\frac{1}{2}}^n = \frac{(-B_x B_{yj}^n + C_{2,j+\frac{1}{2}} v_j^n) + (-B_x B_{yj+1}^n - C_{2,j+\frac{1}{2}} v_{j+1}^n)}{2\mu} \\ (f_6)_{j+\frac{1}{2}}^n = \frac{(-B_x B_{zj}^n + C_{3,j+\frac{1}{2}} w_j^n) + (-B_x B_{zj+1}^n - C_{3,j+\frac{1}{2}} w_{j+1}^n)}{2\mu} \\ (f_7)_{j+\frac{1}{2}}^n = \left[ \frac{(P_{*j}^n + C_{1,j+\frac{1}{2}} u_j^n)^2 - (P_{*j+1}^n - C_{1,j+\frac{1}{2}} u_{j+1}^n)^2}{4C_{1,j+\frac{1}{2}}} \right. \\ \left. + \frac{(-B_x B_{yj}^n + C_{2,j+\frac{1}{2}} v_j^n)^2 - (-B_x B_{yj+1}^n - C_{2,j+\frac{1}{2}} v_{j+1}^n)^2}{4C_{2,j+\frac{1}{2}} \mu} \right. \\ \left. + \frac{(-B_x B_{zj}^n + C_{3,j+\frac{1}{2}} w_j^n)^2 - (-B_x B_{zj+1}^n - C_{3,j+\frac{1}{2}} w_{j+1}^n)^2}{4C_{3,j+\frac{1}{2}} \mu} \right]. \end{array} \right. \quad (15)$$

Again, we see that the couples of variables  $(P_*, u)$ ,  $(B_y, v)$ , and  $(B_z, w)$  are connected: here, they are linked by the three coefficients  $C_1$ ,  $C_2$ , and  $C_3$ . We know that for every choice of the constants  $C_{1,j+1/2}$ ,  $C_{2,j+1/2}$ , and  $C_{3,j+1/2}$ , under a CFL condition, the scheme is entropic. So, to simplify, we propose to choose

$$C_{1,j+\frac{1}{2}} = C_{2,j+\frac{1}{2}} = C_{3,j+\frac{1}{2}} = \max(|\lambda_{i,j}|, |\lambda_{i,j+1}|), \quad (16)$$

where  $\lambda_{i,j}$  are the eigenvalues of the Jacobian matrix  $\frac{df(U)}{dU}(U_j)$ . We know that system (6) is hyperbolic with seven real eigenvalues

$$0, \quad \pm \frac{c_f}{\tau}, \quad \pm \frac{c_a}{\tau}, \quad \pm \frac{c_s}{\tau},$$

corresponding to three MHD waves: fast waves, slow waves, and Alfvén waves. They are defined by

$$\left\{ \begin{array}{l} c_a^2 = \frac{\tau B_z^2}{\mu}, \\ c_f^2 = \frac{1}{2} \left( (a^*)^2 + \sqrt{(a^*)^4 - 4a^2 \frac{\tau B_z^2}{\mu}} \right), \\ c_s^2 = \frac{1}{2} \left( (a^*)^2 - \sqrt{(a^*)^4 - 4a^2 \frac{\tau B_z^2}{\mu}} \right), \end{array} \right. \quad (17)$$

with

$$\begin{cases} a = \tau \sqrt{p \frac{\partial p}{\partial \varepsilon} - \frac{\partial p}{\partial \tau}}, \\ (a^*)^2 = a^2 + \frac{\tau (B_x^2 + B_y^2 + B_z^2)}{\mu}. \end{cases} \quad (18)$$

### 3.4. Comparison with the Roe Scheme

We demonstrate in this section that if the field  $\mathbf{B}$  is vanishing, the Roe scheme and the preceding particular scheme are similar and if not, they define different schemes. Then, on numerical examples, we will compare both. We remind the reader of the definition and some well known properties of the Roe scheme.

The resolution of the Riemann problem

$$\begin{cases} \frac{\partial U}{\partial t} + \frac{\partial f(U)}{\partial m} = 0 \\ U(m, 0) = U_l & \text{if } m < 0 \\ U(m, 0) = U_r & \text{if } m \geq 0 \end{cases}$$

is replaced by the resolution of the linearized Riemann problem

$$\begin{cases} \frac{\partial U}{\partial t} + A(U_l, U_r) \frac{\partial U}{\partial m} = 0 \\ U(m, 0) = U_l & \text{if } m < 0 \\ U(m, 0) = U_r & \text{if } m \geq 0. \end{cases}$$

Here, the Roe matrix  $A(U_l, U_r)$  is required to be consistent with the Jacobian matrix,  $A(U, U) = \frac{df(U)}{dU}$ , to have real eigenvalues and a set of linearly independent eigenvectors, and to satisfy

$$f(U_r) - f(U_l) = A(U_l, U_r)(U_r - U_l).$$

The linearized Riemann problem has a solution composed of eight states separated by seven discontinuity lines. We note that  $(\lambda_j)_{j=1\dots 7}$  the eigenvalues of  $A(U_l, U_r)$ ,  $(V_j)_{j=1\dots 7}$  the associated right eigenvectors, and  $(\beta_j)_{j=1\dots 7}$  are defined by

$$U_r - U_l = \sum_{i=1}^{i=7} \beta_i V_i.$$

The scheme is written in conservative form (11) and the numerical flux is given by

$$G_{roe}(U_l, U_r) = \frac{1}{2}(f(U_l) + f(U_r)) - \frac{1}{2} \sum_{i=1}^{i=7} |\lambda_i| \beta_i V_i.$$

In the following, for each variable  $\alpha$ , we note  $\bar{\alpha} = (\alpha_l + \alpha_r)/2$  and  $\Delta\alpha = \alpha_r - \alpha_l$ . The coefficient  $\tilde{p}_\tau$  is an evaluation of  $(\frac{\partial p}{\partial \tau})_\varepsilon$  and  $\tilde{p}_\varepsilon$  is an evaluation of  $(\frac{\partial p}{\partial \varepsilon})_\tau$ .

*3.4.1. The case of a vanishing magnetic field.* Suppose that  $B_x = 0$  and  $\bar{B}_y^2 + \bar{B}_z^2 = 0$ . The system degenerates to the system of hydrodynamics. We note

$$\frac{\bar{c}^2}{\bar{\tau}^2} = - \left( \frac{\partial p}{\partial \tau} \right)_\xi (\bar{\tau}, \bar{\varepsilon}) \quad \text{with } \bar{\varepsilon} = \frac{\bar{p}\bar{\tau}}{\gamma - 1}.$$

The roe matrix  $A(U_l, U_r)$  has two eigenvalues different from zero,  $\lambda_1 = -\bar{c}/\bar{\tau}$  and  $\lambda_7 = \bar{c}/\bar{\tau}$ , with the eigenvectors

$$V_1 = \begin{pmatrix} \frac{\bar{c}^2}{\bar{\tau}} \\ 0 \\ 0 \\ -\lambda_1 \frac{\bar{c}^2}{\bar{\tau}} \\ 0 \\ 0 \\ -\frac{\bar{c}^2}{\bar{\tau}}(\lambda_1 \bar{u} + \bar{p}) \end{pmatrix}, \quad V_7 = \begin{pmatrix} \frac{\bar{c}^2}{\bar{\tau}} \\ 0 \\ 0 \\ -\lambda_7 \frac{\bar{c}^2}{\bar{\tau}} \\ 0 \\ 0 \\ -\frac{\bar{c}^2}{\bar{\tau}}(\lambda_7 \bar{u} + \bar{p}) \end{pmatrix}$$

and

$$\beta_7 + \beta_1 = -\frac{\bar{\tau} \Delta p}{\bar{c}^2(\bar{p} \bar{p}_\varepsilon - \bar{p}_\tau)}, \quad \beta_7 - \beta_1 = -\frac{\bar{\tau}^2 \Delta u}{\bar{c}^3}.$$

It is not necessary to make explicit here a complete set of eigenvectors to obtain the numerical flux; see [3] for the complete set. Thus, we obtain the lemma

**LEMMA 3.2.** *In the case where  $B_x$  and  $\bar{B}_y^2 + \bar{B}_z^2 = 0$ , the numerical flux of the Roe scheme and the numerical flux given by (12) are identical if  $C_1 = \bar{c}/\bar{\tau}$ .*

*Proof.* We have just to compare the first line, the fourth line, and the last line of the numerical flux. The other lines are zero. The first line of the numerical flux of the Roe scheme is given by

$$\begin{aligned} G_{roe,1}(U_l, U_r) &= -\frac{u_l + u_r}{2} - \frac{1}{2} \frac{\bar{c}^3}{\bar{\tau}^2} (\beta_7 + \beta_1) \\ &= -\frac{u_l + u_r}{2} + \frac{1}{2} \frac{\bar{\tau} \Delta p}{\bar{c}}. \end{aligned}$$

If  $C_{1,j+1/2} = \bar{c}/\bar{\tau}$ , then  $G_{roe,1}(U_j^n, U_{j+1}^n) = (f_1)_{j+1/2}^n$ . The fourth line is given by

$$\begin{aligned} G_{roe,4}(U_l, U_r) &= \frac{p_l + p_r}{2} + \frac{1}{2} \left( \frac{\bar{c}^4}{\bar{\tau}^3} (\beta_7 - \beta_1) \right) \\ &= \frac{p_l + p_r}{2} - \frac{1}{2} \frac{\bar{c} \Delta u}{\bar{\tau}}. \end{aligned}$$

If  $C_{1,j+1/2} = \bar{c}/\bar{\tau}$ , then  $G_{roe,4}(U_j^n, U_{j+1}^n) = (f_4)_{j+1/2}^n$ . The last line can be written

$$\begin{aligned} G_{roe,7}(U_l, U_r) &= \frac{u_l p_l + u_r p_r}{2} - \frac{1}{2} \left( \beta_1 \frac{\bar{c}^3}{\bar{\tau}^2} \left( \frac{\bar{c}}{\bar{\tau}} \bar{u} - \bar{p} \right) + \beta_7 \frac{\bar{c}^3}{\bar{\tau}^2} \left( -\frac{\bar{c}}{\bar{\tau}} \bar{u} - \bar{p} \right) \right) \\ &= \frac{u_l p_l + u_r p_r}{2} - \frac{1}{2} \left( \frac{\bar{c}^4}{\bar{\tau}^3} \bar{u} (\beta_1 - \beta_7) - \frac{\bar{c}^3}{\bar{\tau}^2} \bar{p} (\beta_7 + \beta_1) \right) \\ &= \frac{u_l p_l + u_r p_r}{2} - \frac{1}{2} \left( \frac{\bar{c} \bar{u} \Delta u}{\bar{\tau}} + \frac{\bar{\tau} \bar{p} \Delta p}{\bar{c}} \right). \end{aligned}$$

If  $C_{1,j+1/2} = \bar{c}/\bar{\tau}$ , then  $G_{roe,7}(U_j^n, U_{j+1}^n) = (f_7)_{j+1/2}^n$ . We conclude that if  $C_{1,j+1/2} = \bar{c}/\bar{\tau}$ , then  $G_{roe}(U_j^n, U_{j+1}^n) = f(U)_{j+1/2}^n$ . ■

We can make the following remarks:

*Remark 3.2* (1) This proof is still true when  $B_x = 0$  and  $\bar{B}_y^2 + \bar{B}_z^2 \neq 0$  because in this case, the system of MHD equations degenerates to the system of Euler equations if we replace  $p$  with  $P_*$ .

(2) In the case where  $B_x \neq 0$  and  $\bar{B}_y^2 + \bar{B}_z^2 = 0$ , we can exhibit another set of eigenvectors. We know that in this case, the Alfvén waves are of order of multiplicity 2 or 3. Hence, we can prove that the numerical flux of the Roe scheme and the numerical flux given by (12) are identical if we choose  $C_1 = \tilde{c}_f/\bar{\tau}$ ,  $C_2 = \tilde{c}_a/\bar{\tau}$ , and  $C_3 = \tilde{c}_s/\bar{\tau}$ .

(3) In the cases presented here, both numerical fluxes are equal. So, we can deduce that in these cases, the Roe scheme satisfies also an entropy inequality under a CFL condition. Nevertheless, we know that the approximate Riemann solver of Roe can calculate unphysical intermediate states, especially in regions of strong compressions. Let us exhibit such an example. In [20], Munz demonstrates that for the Riemann problem given by Eq. (1) and the initial conditions

$$U(m, 0) = \begin{cases} U_l = (\tau_0, 0, 0, u_0, v_0, w_0, E_0)^t & \text{for } m < 0 \\ U_r = (\tau_0, 0, 0, -u_0, v_0, w_0, E_0)^t & \text{for } m > 0 \end{cases}$$

with  $u_0 > 0$ , the Roe linearization fails if

$$\frac{u_0}{c_0} > 1$$

and  $c_0 = \sqrt{\gamma p_0 \tau_0}$  is the Eulerian speed of sound. In this case, the intermediate density calculated by the Roe solver becomes negative.

*3.4.2. The case of a non-vanishing magnetic field.* We suppose that  $B_x \neq 0$  and  $\bar{B}_y^2 + \bar{B}_z^2 \neq 0$ . We adopt the notations

$$\begin{aligned} \tilde{a} &= \bar{\tau} \sqrt{\tilde{p} \tilde{p}_\varepsilon - \tilde{p}_\tau} \\ \tilde{b}_x &= \sqrt{\frac{B_x^2 \bar{\tau}}{\mu}} \quad \text{and} \quad \tilde{b} = \sqrt{\frac{\bar{B}^2 \bar{\tau}}{\mu}} \\ (\tilde{a}^*)^2 &= \tilde{a}^2 + \tilde{b}^2 \end{aligned}$$

with

$$\tilde{p} = \bar{p} + \frac{1}{4\mu} ((\Delta B_y)^2 + (\Delta B_z)^2).$$

The matrix  $A(U_l, U_r)$  has seven eigenvalues ordered

$$\lambda_1 = -\frac{\tilde{c}_f}{\bar{\tau}}, \lambda_2 = -\frac{\tilde{c}_a}{\bar{\tau}}, \lambda_3 = -\frac{\tilde{c}_s}{\bar{\tau}}, \lambda_4 = 0, \lambda_5 = \frac{\tilde{c}_s}{\bar{\tau}}, \lambda_6 = \frac{\tilde{c}_a}{\bar{\tau}}, \lambda_7 = \frac{\tilde{c}_f}{\bar{\tau}}$$

with

$$\begin{cases} \tilde{c}_a = \tilde{b}_x \\ \tilde{c}_s = \sqrt{\frac{1}{2}((\tilde{a}^*)^2 - \sqrt{(\tilde{a}^*)^4 - 4\tilde{a}^2\tilde{b}_x^2})} \\ \tilde{c}_f = \sqrt{\frac{1}{2}((\tilde{a}^*)^2 + \sqrt{(\tilde{a}^*)^4 - 4\tilde{a}^2\tilde{b}_x^2})} \end{cases}$$



The coefficients  $\beta_i$  are the coefficients of decomposition of  $U_r - U_l$  on the set of eigenvectors and we introduce

$$\begin{cases} \gamma_f^+ = \beta_7 + \beta_1 \\ \gamma_f^- = \beta_7 - \beta_1 \\ \gamma_s^+ = \beta_5 + \beta_3 \\ \gamma_s^- = \beta_5 - \beta_3 \\ \gamma_a^+ = \beta_6 + \beta_2 \\ \gamma_a^- = \beta_6 - \beta_2. \end{cases}$$

We note

$$\delta_s = \frac{\tilde{c}_s^2}{\tilde{\tau}} - \frac{B_x^2}{\mu} = \frac{1}{\tilde{\tau}}(\tilde{c}_s^2 - \tilde{c}_a^2), \quad \delta_f = \frac{\tilde{c}_f^2}{\tilde{\tau}} - \frac{B_x^2}{\mu} = \frac{1}{\tilde{\tau}}(\tilde{c}_f^2 - \tilde{c}_a^2)$$

and

$$s = \begin{cases} \text{sgn}(B_x) & \text{if } B_x \neq 0 \\ 0 & \text{if not.} \end{cases}$$

We obtain the set of eigenvectors

$$V_1 = \begin{bmatrix} \delta_f \\ -\frac{B_x^2 \bar{B}_y}{\mu} \\ -\frac{B_x^2 \bar{B}_z}{\mu} \\ -\lambda_1 \delta_f \\ \lambda_1 \frac{B_x \bar{B}_y}{\mu} \\ \lambda_1 \frac{B_x \bar{B}_z}{\mu} \\ \alpha_1 \end{bmatrix}, \quad V_2 = \begin{bmatrix} 0 \\ -s \bar{B}_z \sqrt{\tilde{\tau} \mu} \\ s \bar{B}_y \sqrt{\tilde{\tau} \mu} \\ 0 \\ -\bar{B}_z \\ \bar{B}_y \\ -(\bar{B}_z \bar{v} - \bar{B}_y \bar{w}) \end{bmatrix}, \quad V_3 = \begin{bmatrix} \delta_s \\ -\frac{B_x^2 \bar{B}_y}{\mu} \\ -\frac{B_x^2 \bar{B}_z}{\mu} \\ -\lambda_3 \delta_s \\ \lambda_3 \frac{B_x \bar{B}_y}{\mu} \\ \lambda_3 \frac{B_x \bar{B}_z}{\mu} \\ \alpha_3 \end{bmatrix},$$

$$V_4 = - \begin{bmatrix} \tilde{p}_\varepsilon \\ \tilde{p}_\varepsilon \bar{B}_y \\ \tilde{p}_\varepsilon \bar{B}_z \\ 0 \\ 0 \\ 0 \\ \tilde{p}_\varepsilon \frac{\bar{B}^2}{2\mu} - \tilde{p}_\tau \end{bmatrix},$$

$$V_5 = \begin{bmatrix} \delta_s \\ -\frac{B_x^2 \bar{B}_y}{\mu} \\ -\frac{B_x^2 \bar{B}_z}{\mu} \\ -\lambda_5 \delta_s \\ \lambda_5 \frac{B_x \bar{B}_y}{\mu} \\ \lambda_5 \frac{B_x \bar{B}_z}{\mu} \\ \alpha_5 \end{bmatrix}, \quad V_6 = \begin{bmatrix} 0 \\ -s \bar{B}_z \sqrt{\bar{\tau} \mu} \\ s \bar{B}_y \sqrt{\bar{\tau} \mu} \\ 0 \\ \bar{B}_z \\ -\bar{B}_y \\ (\bar{B}_z \bar{v} - \bar{B}_y \bar{w}) \end{bmatrix}, \quad \text{and} \quad V_7 = \begin{bmatrix} \delta_f \\ -\frac{B_x^2 \bar{B}_y}{\mu} \\ -\frac{B_x^2 \bar{B}_z}{\mu} \\ -\lambda_7 \delta_f \\ \lambda_7 \frac{B_x \bar{B}_y}{\mu} \\ \lambda_7 \frac{B_x \bar{B}_z}{\mu} \\ \alpha_7 \end{bmatrix},$$

with

$$\begin{cases} \alpha_i = \delta_s \left( \frac{\bar{B}^2}{2\mu} - \lambda_i \bar{u} - \bar{p} \right) - \lambda_i^2 \frac{\bar{\tau}}{\mu} (\bar{B}_y^2 + \bar{B}_z^2) + \lambda_i \frac{B_x}{\mu} (\bar{v} \bar{B}_y + \bar{w} \bar{B}_z) & \text{for } i \in \{3, 5\}, \\ \alpha_j = \delta_f \left( \frac{\bar{B}^2}{2\mu} - \lambda_j \bar{u} - \bar{p} \right) - \lambda_j^2 \frac{\bar{\tau}}{\mu} (\bar{B}_y^2 + \bar{B}_z^2) + \lambda_j \frac{B_x}{\mu} (\bar{v} \bar{B}_y + \bar{w} \bar{B}_z) & \text{for } j \in \{1, 7\}. \end{cases}$$

The coefficients of decomposition on the set of eigenvectors are given by

$$\begin{aligned} \beta_4 &= \frac{\tilde{p} \Delta \tau + \Delta \varepsilon}{\tilde{p}_\tau - \tilde{p} \tilde{p}_\varepsilon}, \\ \gamma_a^+ &= -\frac{\sqrt{\bar{\tau}}}{s \sqrt{\mu} (\bar{B}_y^2 + \bar{B}_z^2)} (\bar{B}_y \Delta B_z - \bar{B}_z \Delta B_y), \\ \gamma_f^+ &= \frac{1}{\delta_f \tilde{c}_s^2 - \delta_s \tilde{c}_f^2} \left( \frac{\tilde{c}_s^2 \Delta p}{\tilde{p}_\tau - \tilde{p} \tilde{p}_\varepsilon} + \frac{\delta_s \bar{\tau}^2}{\bar{B}_y^2 + \bar{B}_z^2} (\bar{B}_y \Delta B_y + \bar{B}_z \Delta B_z) \right), \\ \gamma_s^+ &= \frac{1}{\delta_s \tilde{c}_f^2 - \delta_f \tilde{c}_s^2} \left( \frac{\tilde{c}_f^2 \Delta p}{\tilde{p}_\tau - \tilde{p} \tilde{p}_\varepsilon} + \frac{\delta_f \bar{\tau}^2}{\bar{B}_y^2 + \bar{B}_z^2} (\bar{B}_y \Delta B_y + \bar{B}_z \Delta B_z) \right), \\ \gamma_a^- &= \frac{1}{\bar{B}_y^2 + \bar{B}_z^2} (\bar{B}_z \Delta v - \bar{B}_y \Delta w), \\ \gamma_f^- &= \frac{\bar{\tau}}{\tilde{c}_f (\delta_s - \delta_f)} \left( \Delta u + \frac{\delta_s \mu}{B_x} \frac{\bar{B}_z \Delta w + \bar{B}_y \Delta v}{\bar{B}_y^2 + \bar{B}_z^2} \right), \\ \gamma_s^- &= \frac{\bar{\tau}}{\tilde{c}_s (\delta_f - \delta_s)} \left( \Delta u + \frac{\delta_f \mu}{B_x} \frac{\bar{B}_z \Delta w + \bar{B}_y \Delta v}{\bar{B}_y^2 + \bar{B}_z^2} \right). \end{aligned}$$

We can demonstrate the following lemma

**LEMMA 3.3.** *In the case where  $B_x \neq 0$  and  $\bar{B}_y^2 + \bar{B}_z^2 = 0$ , the Roe scheme and the scheme given by the numerical flux (12) are different.*

*Proof.* It is sufficient to demonstrate that the fifth component of both numerical fluxes is different when the magnetic field is non-zero.

$$\begin{aligned}
& G_{roe,5}(U_l, U_r) \\
&= -\frac{B_x}{2}(B_{yl} + B_{yr}) - \frac{1}{2} \left( \frac{\tilde{c}_f^2}{\tilde{\tau}^2} \frac{B_x \bar{B}_y}{\mu} (\beta_7 - \beta_1) + \frac{\tilde{c}_s^2}{\tilde{\tau}^2} \frac{B_x \bar{B}_y}{\mu} (\beta_5 - \beta_3) + \frac{\tilde{c}_a}{\tilde{\tau}} \bar{B}_z (\beta_6 - \beta_2) \right) \\
&= -\frac{B_x}{2}(B_{yl} + B_{yr}) - \frac{1}{2} \left( \frac{\tilde{c}_f^2}{\tilde{\tau}^2} \frac{B_x \bar{B}_y}{\mu} \gamma_f^- + \frac{\tilde{c}_s^2}{\tilde{\tau}^2} \frac{B_x \bar{B}_y}{\mu} \gamma_s^- + \frac{\tilde{c}_a}{\tilde{\tau}} \bar{B}_z \gamma_a^- \right) \\
&= -\frac{B_x}{2}(B_{yl} + B_{yr}) - \frac{1}{2} (\alpha_1 \Delta u + \alpha_2 \Delta v + \alpha_3 \Delta w),
\end{aligned}$$

where  $\alpha_1$ ,  $\alpha_2$ , and  $\alpha_3$  are coefficients. Let us calculate  $\alpha_1$ ,

$$\begin{aligned}
\alpha_1 &= \frac{c_f^2}{\tau^2} \frac{B_x \bar{B}_y}{\mu} \frac{\bar{\tau}}{\tilde{c}_f(\delta_s - \delta_f)} - \frac{c_s^2}{\tau^2} \frac{B_x \bar{B}_y}{\mu} \frac{\bar{\tau}}{\tilde{c}_s(\delta_s - \delta_f)} \\
&= \frac{B_x \bar{B}_y}{\mu} \left( \frac{\tilde{c}_f/\bar{\tau} - \tilde{c}_s/\bar{\tau}}{\delta_s - \delta_f} \right).
\end{aligned}$$

This coefficient  $\alpha_1$  is non-zero when  $B_x \neq 0$  and  $\bar{B}_y^2 + \bar{B}_z^2 \neq 0$ . If we look at the numerical flux given by (12), we see that  $f_5$  is independent of  $\Delta u$  and only depends on  $\Delta v$ . Then, we deduce that both schemes are different. ■

In the next section, we will propose examples to compare both schemes.

#### 4. NUMERICAL APPLICATIONS OF THE SCHEME

In this section, we present the robustness and accuracy of the particular scheme described in the previous section through numerical examples. We propose various shock tube problems which will be composed of all (or a part of) the MHD waves. We compare our results with results obtained by other approximate Riemann solvers, in particular with the Roe solver. The same scheme is used to compare both solvers. To test this scheme, we have used a lagrangian one-dimensional code and we only propose results of order one in space and time. The values of left and right states for the following test cases are inspired by the work [5–7] except that following [7] we take  $\gamma = 1.4$ . As noticed in [7] the numerical solution with  $\gamma = 1.4$  is very close to the numerical solution with  $\gamma = 2$  [5]. The CFL number is 0.9 with the constant set according to formula (16).

Let us emphasize that the discussion of numerical results is a subtle task for ideal MHD, even in 1D. We will see this for the third test case.

##### 4.1. Shock Tube 1: A Coplanar Riemann Problem without Normal Magnetic Field

For this case, initial conditions are  $(\rho, u, v, w, B_x, B_y, B_z, p)_l = (1, 0, 0, 0, 0, 1, 0, 1000)$  for  $0 \leq x \leq 100$  and  $(\rho, u, v, w, B_x, B_y, B_z, p)_r = (0.125, 0, 0, 0, 0, -1, 0, 0.1)$  for  $100 \leq x \leq 200$ . We take 800 points on a length discretization of 200 and we show the solution at time  $t = 1.4$ . In this case, the longitudinal component of the magnetic field vanishes. Consequently, the system of MHD equations reduces to the system of gas dynamics with a new pressure law given by  $p^* = p + B^2/2\mu$ .

We notice that Alfvén waves and slow waves vanish. This problem is composed of a fast rarefaction going to the left, a fast shock going to the right, and a tangential discontinuity

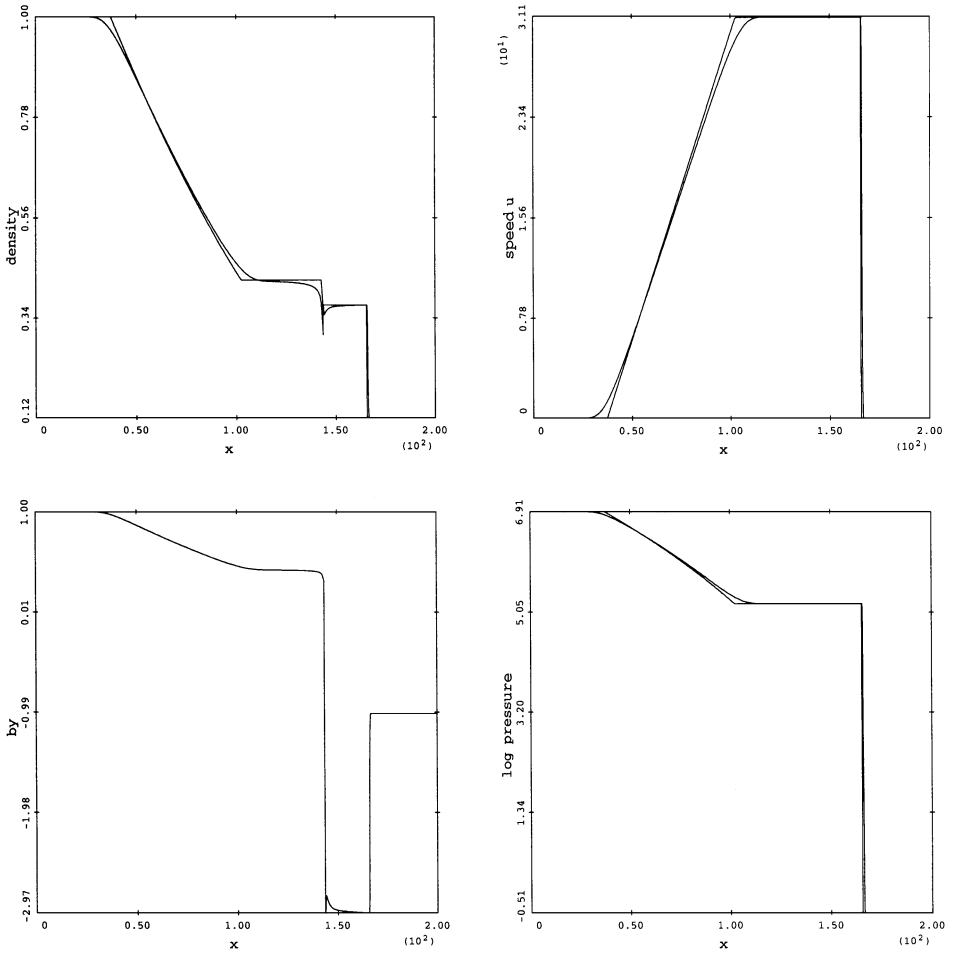


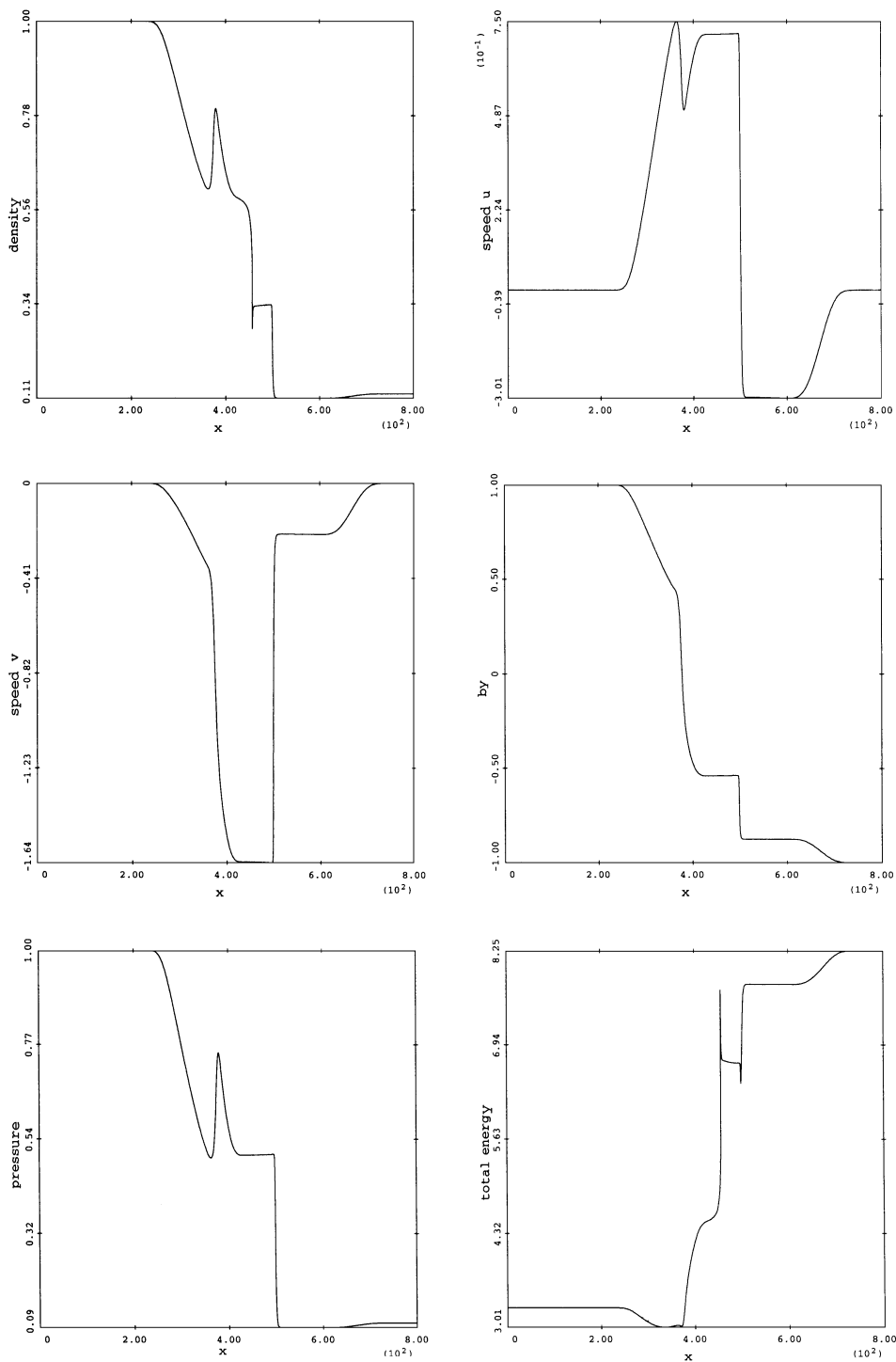
FIG. 1. Shock tube 1, order 1.

which is a contact discontinuity through which  $p^*$  is kept. Results are given in Fig. 1 and are compared to the exact solution. We can observe an undershoot at the contact discontinuity on the density profile: it is a frequent shortcoming of lagrangian codes sometimes called “wall heating.” These results are satisfying and very similar to the results from a Roe solver. The comparisons with a Roe solver are not presented here because we can’t see any differences on the pictures.

#### 4.2. Shock Tube 2: A Coplanar Riemann Problem with Normal Magnetic Field

Initial conditions are  $(\rho, u, v, w, B_x, B_y, B_z, p)_l = (1, 0, 0, 0, 0.75, 1, 0, 1)$  for  $0 \leq x \leq 400$  and  $(\rho, u, v, w, B_x, B_y, B_z, p)_r = (0.125, 0, 0, 0, 0.75, -1, 0, 0.1)$  for  $400 \leq x \leq 800$ . We take 800 points on a length discretization of 800 and we show the solution at time  $t = 80$ .

In this case, we observe a fast rarefaction propagating to the left, a compound wave composed of an intermediate shock and a slow rarefaction going to the left, a contact discontinuity, a slow shock going to the right, and a fast rarefaction wave going to the right. Results are proposed in Fig. 2. We recognize on the density profile each wave very precisely. Again, we notice an undershoot at the contact discontinuity. Here, it is more interesting to

**FIG. 2.** Shock tube 2, order 1.

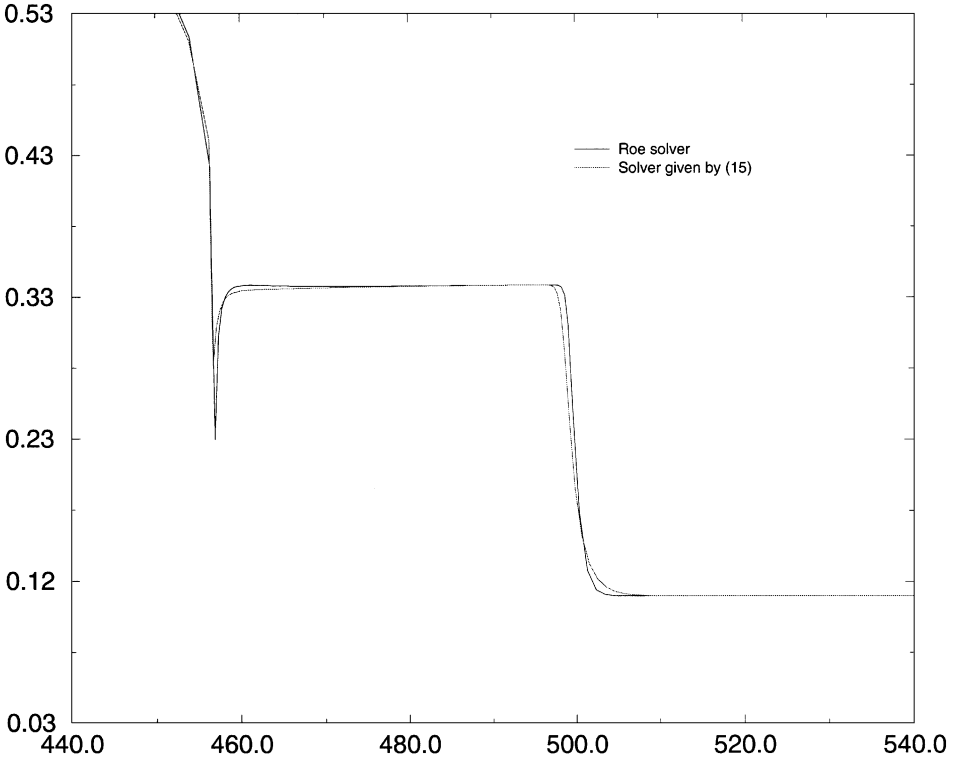


**FIG. 3.** Comparison of the solver given by (15) and the Roe scheme, Shock tube 2, order 1. The stiffest profile is provided by the Roe scheme.

compare the results with another approximate Riemann solver: a Roe solver. We propose both results in Fig. 3 which represents a detail of the density near the contact discontinuity. We notice that the Roe solver is more precise on the contact discontinuity, otherwise, the results are still very similar.

#### 4.3. Shock Tube 3

In this last case, the  $z$ -component of the magnetic field is not zero. Initial conditions are given by  $(\rho, u, v, w, B_x, B_y, B_z, p)_l = (1, 0, 0, 0, 0.75, 1, 2, 1)$  for  $0 \leq x \leq 400$  and  $(\rho, u, v, w, B_x, B_y, B_z, p)_r = (0.125, 0, 0, 0, 0.75, -1, 1, 0.1)$  for  $400 \leq x \leq 800$ . We take 800 points on a length discretization of 800 and we show the solution at time  $t = 60$ .

This test case presents the following waves: a fast rarefaction to the left, a slow wave to the left, a contact discontinuity, a slow shock to the right, a fast shock to the right, and two Alfvén waves visible on the transverse components of the velocity and of the magnetic field. This case is of particular interest since seven distinct waves are propagating, especially the Alfvén waves missing from the other test cases. Results are presented in Fig. 4. We can see quite precisely each wave propagating on the different profiles. Here, the comparison with the Roe solver shows that the Roe solver treats the stiffness of the discontinuities in the solution better than the conservative solver: this is quite clear in Fig. 5. Nevertheless, both results give a coherent solution. This was also reported in [6] using high order different solvers.

It is striking to observe that we may conclude abusively from the numerical results that the slow wave to the left is a slow compound wave. This numerical artifact has also been

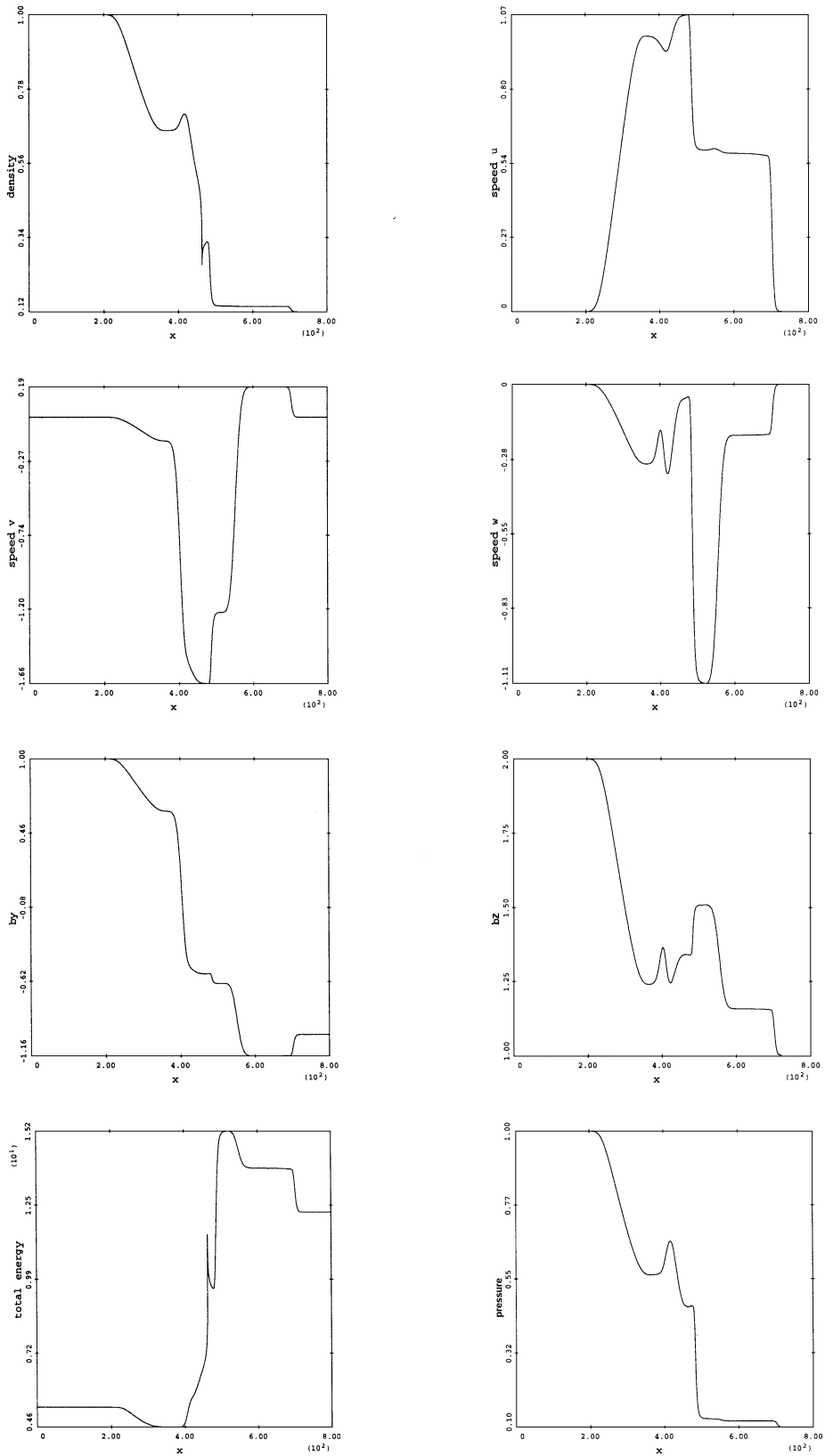
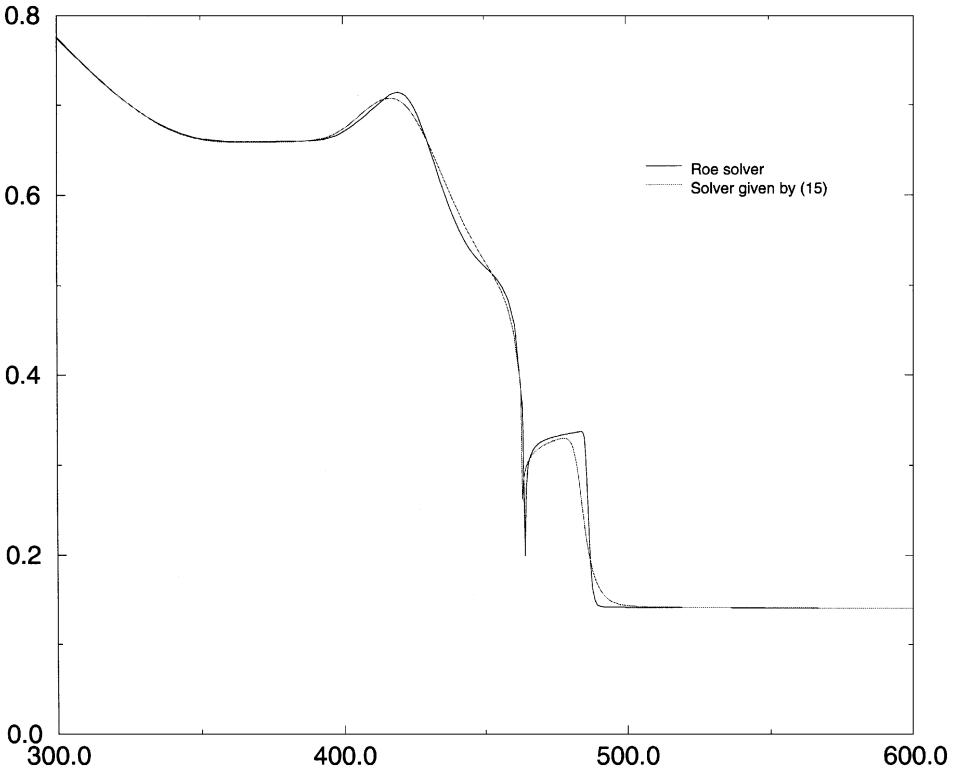


FIG. 4. Shock tube 3, order 1.



**FIG. 5.** Comparison of densities given by scheme (15) and the Roe scheme, Shock tube 3, order 1. The stiffest profile is provided by the Roe scheme.

reported in [6] using other solvers and refined meshes. Nevertheless following [2] such a wave is excluded on theoretical grounds. So there is probably no compound wave in that case. We also refer to [18, 19] for numerical and theoretical investigation of a non-coplanar Riemann problem in MHD and related problems. It seems to us that a deep understanding of these non-coplanar numerical Riemann problems in MHD is not really achieved nowadays. Moreover the question is far from the scope of this paper. So we do not follow further our interpretation of the numerical results of this test case, which was designed mainly to compare both solvers.

## 5. CONCLUSION

In this paper, we have shown that the lagrangian one-dimensional MHD equations satisfy some particular properties, shared with other systems of conservation laws with vanishing entropy flux. These properties are used to construct a class of entropic numerical schemes. We present here a particular scheme of this class. Numerically, this scheme behaves well. In the tests presented here, we can observe the phenomenon of “wall heating” at the contact discontinuity: this is an undershoot characteristic of a lagrangian calculation and it isn’t linked with the scheme itself.

This scheme has been compared with other approximate Riemann solvers. In the section of numerical results, we have presented a few comparisons with the Roe scheme. They look similar in cases where one component (longitudinal or transverse) of the magnetic field vanishes. The conclusion of this comparison is that we have quite the same behavior for



both schemes. But, the scheme presented here is far more interesting because it is very easy to compute and it satisfies good properties. Comparatively, the Roe scheme requires the knowledge of a set of eigenvectors.

We are now working on a full extension to 3D ideal MHD, with careful attention paid to the free divergence constraint on the magnetic field. This will be the subject of a forthcoming paper.

### ACKNOWLEDGMENT

The authors deeply thank the referees for their kind remarks. The rigor of the analysis of the numerical results has taken great advantage of these remarks.

### REFERENCES

1. F. Angrand, *Méthode numérique pour la MHD idéale eulérienne de type FLIP*, Technical Report, 1996.
2. Barmin, Kulikovskiy, and Pogorelov, Shock-capturing approach and nonevolutionary solutions in magneto-hydrodynamics, *J. Comput. Phys.* **126**, 77 (1996).
3. F. Beazard, *Approximation numérique de problèmes d'interfaces en mécanique des fluides*, Ph.D. thesis, Ecole Polytechnique, France, 1998.
4. G. Boillat, Symétrisation des systèmes d'équations aux dérivées partielles avec densité d'énergie convexe et contraintes, *C. R. Acad. Sci. Paris* **295**, 551 (1982).
5. M. Brio and C.-C. Wu, An upwind differencing scheme for the equations of ideal magnetohydrodynamics, *J. Comput. Phys.* **75**, 400 (1988).
6. P. Cargo, *Nouveaux modèles numériques pour l'hydrodynamique atmosphérique et la magnétohydrodynamique idéale*, Ph.D. thesis, University Bordeaux I, France, 1995.
7. P. Cargo and G. Gallice, Roe matrices for ideal MHD and systematic construction of Roe matrices for systems of conservation laws, *J. Comput. Phys.* **136**, 446 (1997).
8. P. Cargo, G. Gallice, and P.-A. Raviart, Construction d'une linéarisée de Roe pour les équations de la MHD idéale, *C. R. Acad. Sci. Paris Sér. I* **323**, 951 (1996).
9. W. Dai and P.-R. Woodward, An approximate Riemann solver for ideal magnetohydrodynamics, *J. Comput. Phys.* **111**, 354 (1994).
10. W. Dai and P.-R. Woodward, A high-order Godunov-type scheme for shock interactions in ideal magnetohydrodynamics, *SIAM J. Sci. Comput.* **18**, 957 (1997).
11. B. Després, Structure des systèmes de lois de conservation en variables Lagrangiennes, *C. R. Acad. Sci. Paris*, in press.
12. B. Després, Inégalité entropique pour un solveur conservatif du système de la dynamique des gaz en coordonnées de Lagrange, *C. R. Acad. Sci. Paris Sér. I* **324**, 1301 (1997).
13. B. Després, Structure of lagrangian systems of conservation laws, approximate Riemann solvers and the entropy condition, *Numer. Math.*, in press.
14. E. Godlewski and P.-A. Raviart, *Hyperbolic Systems of Conservation Laws* (Soc. for Industr. & Appl. Math., Philadelphia, 1991).
15. E. Godlewski and P.-A. Raviart, *Numerical Approximation of Hyperbolic Systems of Conservation Laws* (Springer-Verlag, New York/Berlin, 1996).
16. R. Khanfir, *Approximation volumes finis de type cinétique du système hyperbolique de la MHD idéale compressible à pression isotrope*, Thèse, 1995.
17. L. Landau and F. Lifchitz, *Électrodynamique des milieux continus* (Mir, Moscow, 1969), Vol. 8.
18. Y. Lin, L.-C. Lee, and C.-F. Kennel, *Geophys. Res. Lett.* **19**(3), 229 (1992).
19. C.-C. Wu and C.-F. Kennel, *Phys. Fluids B* **5**(8), 2877 (1993).
20. C.-D. Munz, On Godunov-type schemes for Lagrangian gas dynamics, *SIAM J. Numer. Anal.* **31**, 17 (1994).
21. P.-A. Raviart, Méthode Pic pour la MHD, to appear.